ARCHIVIO ISTITUZIONALE
DELLA RICERCA

Alma Mater Studiorum Università di Bologna
Archivio istituzionale della ricerca

A Thorough Analysis of Radio Resource Assignment for UAV-Enhanced Vehicular Sidelink Communications

This is the final peer-reviewed author's accepted manuscript (postprint) of the following publication:

Published Version:
Conserva, F., Linsalata, F., Mizmizi, M., Magarini, M., Spagnolini, U., Verdone, R., et al. (2024). A Thorough Analysis of Radio Resource Assignment for UAV-Enhanced Vehicular Sidelink Communications. NEW YORK : Institute of Electrical and Electronics Engineers Inc. [10.1109/ICC51166.2024.10622534].

Availability:
This version is available at: https://hdl.handle.net/11585/982374 since: 2026-02-06

Published:
DOI: http://doi.org/10.1109/ICC51166.2024.10622534

Terms of use:

Some rights reserved. The terms and conditions for the reuse of this version of the manuscript are specified in the publishing policy. For all terms of use and more information see the publisher's website.

This item was downloaded from IRIS Università di Bologna (https://cris.unibo.it/).
When citing, please refer to the published version.

(Article begins on next page)

13 May 2026

A Thorough Analysis of Radio Resource Assignment for UAV-Enhanced Vehicular Sidelink Communications

Francesca Conserva*, Francesco Linsalata†, Marouan Mizmizi†, Maurizio Magarini†, Umberto Spagnolini†, Roberto Verdone* and Chiara Buratti*

* Dipartimento di Ingegneria dell'Energia Elettrica e dell'Informazione, University of Bologna, & WiLab, CNIT, *Italy*

† Dipartimento di Elettronica, Informazione e Bioingegneria, Politecnico di Milano, Milan, *Italy*

***Abstract*—The rapid expansion of connected and autonomous vehicles (CAVs) and the shift towards millimiter-wave (mmWave) frequencies offer unprecedented opportunities to enhance road safety and traffic efficiency. Sidelink communication, enabling direct Vehicle-to-Vehicle (V2V) communications, play a pivotal role in this transformation. As communication technologies transit to higher frequencies, the associated increase in bandwidth comes at the cost of a severe path and penetration loss. In response to these challenges, we investigate a network configuration that deploys beamforming-capable Unmanned Aerial Vehicles (UAVs) as relay nodes. In this work, we present a comprehensive analytical framework with a groundbreaking performance metric, i.e. average access probability, that quantifies user satisfaction, considering factors across different protocol stack layers. Additionally, we introduce two Radio Resources Assignment (RRA) methods tailored for UAVs. These methods consider parameters such as resource availability, vehicle distribution, and latency requirements. Through our analytical approach, we optimize the average access probability by controlling UAV altitude based on traffic density. Our numerical findings validate the proposed model and strategy, which ensures that Quality of Service (QoS) standards are met in the domain of Vehicle-to-Anything (V2X) sidelink communications.**

***Index Terms*—Unmanned Aerial Vehicles, V2X, Radio Resource Assignment, Beamforming, QoS.**

I. Introduction

The widespread deployment of CAVs is currently underway, holding the potential to revolutionize global mobility by significantly enhancing road safety and efficiency [1], [2]. Notably, V2X communications, with specific emphasis on sidelink technology, facilitate direct V2V interaction via the PC5 interface [3]. This technological advancement serves as a pivotal enabler for a multitude of vehicular applications, including, but not limited to, extended sensing, cooperative awareness, and coordinated maneuvers [4]. These applications exhibit a considerable demand for data rate, which enforces a shift towards the mmWave spectrum (>24 GHz) to explore the large available bandwidth [5]. However, communication at mmWave frequencies entails using beamforming systems to counteract the severe path and penetration loss associated with the propagation of high-frequency signals. In contexts characterized by high mobility, such as in V2X scenarios, line of sight (LoS) blockages become increasingly prevalent as traffic density rises, consequently posing a substantial challenge to communication reliability [6]. An effective strategy to mitigate this issue is to implement relay-assisted transmissions. Various relay mechanisms have been investigated in the literature, including opportunistic relays, Road Side Units (RSUs), and Intelligent Reflective Surfaces (IRSs) [6]–[8].

Relay-aided communications, particularly leveraging UAVs, have gained significant attention for enhancing various aspects of communication systems [9]–[11]. In the field of Intelligent Transport Systems (ITSs), UAVs can be vital during disasters or network failures. The paper [12] proposes a method for predicting information dissemination through sidelink communication to guide UAV flight trajectories, swiftly disseminating information to vehicles. In [13], the authors explore the potential of utilizing UAVs in vehicular networks for task offloading. Their objective is to maximize the number of offloaded tasks by jointly optimizing the initial UAV launch point and strategically associating CAVs to the UAV. In [14], UAVs are also examined, investigating their utilization for supporting edge caching in terrestrial vehicular networks while maximizing the overall network throughput by formulating a joint caching and trajectory optimization problem. In [15], UAVs serve as relays to mitigate the rapid topology changes impacting vehicular networks, leading to connectivity interruptions and data delivery delays. The authors of [16] address UAV-aided mmWave vehicular networks. Their objective is to minimize time consumption while meeting traffic demands through efficient resource allocation schemes.

These works, although relevant in the context of using UAV as relays, have predominantly focused on providing analytical frameworks limited to specific domains, encompassing connectivity assessment [15], optimal UAV deployment [12], trajectory optimization [12], [14], throughput maximization [14], or relay selection [13].

In this article, we introduce an enhanced approach to sidelink communications by adopting beamforming-enabled UAVs as relay nodes. This ensures the reliable exchange of data on the sidelink data plane, even in scenarios where LoS communication is obstructed. Particularly, building upon [17], our intention is to advance the current state of knowledge by introducing a comprehensive analytical framework that features a novel performance metric: the average access probability. The latter numerically quantifies the average user satisfaction following the RRA process when more CAVs are covered by an UAV

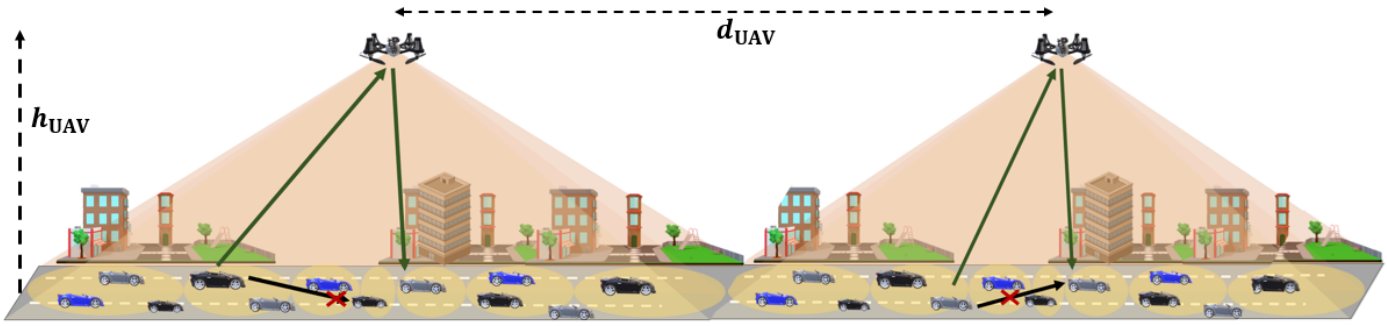

Fig. 1: UAV-Enhanced vehicular sidelink communications scenario: CAVs, seeking to establish communication with other CAVs, but facing a blocked V2V link, exploit UAV as relay.

and request resources to fulfill traffic demand.

In contrast with previous work, our mathematical framework concurrently considers aspects that span across multiple layers of the protocol stack. Specifically, the proposed framework accounts for: i) on-board beamforming; ii) coverage analysis, dealing with the statistics of the Signal-to-Noise Ratio (SNR); iii) radio resource assignment strategies; iv) distribution of underlying vehicles, UAV altitude, available bandwidth and v) application-dependent V2X traffic demand from CAVs. Notably, none of the aforementioned works concentrate on any particular V2X use case while accounting for the high vehicular traffic demand, which is a crucial aspect to manage.

Contributions The main contributions of this research can be summarized as follows:

- An analytical characterization of the average access probability is proposed. This analysis emphasizes the impact of critical system parameters, the RRA process, traffic dynamics, and V2X QoS requirements.
- Two distinct RRA algorithms are also presented. These algorithms consider factors such as vehicle distribution, beamforming, and available bandwidth, resulting in varying performance outcomes depending on the selected scenario.

Organization The remainder of the paper is organized as follows. Section II defines the system model. The RRA algorithms and their performances are characterized in Sec. III. The simulation results are presented in Sec. IV. Lastly, Sec. V concludes the work.

II. System Model

Let us examine the V2V communication scenario supported by UAVs, as illustrated in Figure 1. In this setting, M CAVs are in transit along a highway, while Q UAVs are positioned above the CAVs at an altitude h_{UAV}. The UAVs are evenly distributed along the road at a fixed distance of d_{UAV} from one another, and each UAV is responsible for covering a specific road segment with a length of L_{f}. We assume that each UAV has a hybrid digital Uniform Linear Array (ULA) with N_{UAV} antenna elements and N_{RF} radio-frequency (RF) chains, while each CAV equips an ULA with N_{CAV} antenna elements and a single RF chain. When the ith CAV detects a communication disruption with the jth CAV, a request for relay assistance is initiated and directed towards the qth UAV responsible for covering the road segment corresponding to the ith CAV.

A. UAV Beamforming Design

The UAVs utilize a set of beams, denoted as $\mathcal{B}$, which serves as a codebook for both uplink and downlink operations. Similarly to the 5G NR Standard [18], we assume that each communication instance occurs in a pre-defined time-frequency resource. A scheduling strategy is implemented at the UAV to ensure that CAVs served by the same beam are assigned distinct time-frequency resources to prevent interference, whereas CAVs covered by different beams can share the same time-frequency resources. The association between beams and CAVs can be established during the initial access procedure as in [19].

Since the UAV employs a hybrid digital beamforming (HBF) architecture with N_{RF} chains, for each time-frequency resource, the scheduler allocates N_{RF} CAVs that are simultaneously transmitting towards the UAV. The signal transmitted by the ith CAV is $\mathbf{x}_i = \mathbf{f}_i s_i$, where $\mathbf{f}_i \in \mathbb{C}^{N_{\text{CAV}} \times 1}$ denotes the beamforming vector and s_i denotes the transmitted symbol such that $\mathbb{E}\left[s_i^* s_i\right] = 1$. After time synchronization, the discrete-time signal received by the UAV, in a generic time-frequency resource, can be expressed as

$$\mathbf{y} = \sum_{i=1}^{N_{\text{RF}}} \sqrt{\rho_i}\, \mathbf{H}_i\, \mathbf{x}_i + \mathbf{n}\,, \tag{1}$$

where $\mathbf{H}_i \in \mathbb{C}^{N_{\text{UAV}} \times N_{\text{CAV}}}$ is the channel impulse response such that $\mathbb{E}\left[\|H_i\|_{\text{F}}^2\right] = 1$, $\mathbf{n} \sim \mathcal{CN}(0, \sigma_n^2)$ denotes the additive Gaussian noise, and ρ_i represents the average received power from the ith CAV, defined as

$$\rho_i = \frac{N_{\text{UAV}}\, N_{\text{CAV}}\, P_i}{PL_i}, \tag{2}$$

where P_i denotes the transmitted power and PL_i is the path loss. The signal from the ith CAV decoded at the UAV can be expressed as

$$\hat{s}_i = \sqrt{\rho_i} \mathbf{w}_\ell^{\text{H}}\, \mathbf{H}_i\, \mathbf{x}_i + \mathbf{w}_\ell^{\text{H}}\, \mathbf{n}, \tag{3}$$

where $\mathbf{w}_\ell \in \mathbb{C}^{N_{\text{UAV}} \times 1}$ is the beamforming vector applied at UAV, that is drawn from the codebook $\mathbf{w}_\ell \in \mathcal{B}$. Throughout the paper, we consider a Discrete Fourier Transform (DFT) codebook as in [20], which ensures full coverage with the

minimum number of beams. The resulting instantaneous SNR is given by

$$\mathrm{SNR}_i = \frac{\rho_i \left\| \mathbf{w}_\ell^{\mathrm{H}} \mathbf{H}_i \, \mathbf{f}_i \right\|^2}{\sigma_n^2}. \tag{4}$$

B. Channel Model

The strategic placement of the UAV ensures a reliable ground-to-aerial communication link without obstructions. The path loss in dB experienced by the link from the ith CAV can be expressed as in [21]:

$$PL_i = A + \alpha \, 10 \log_{10}(d_i) + \eta, \tag{5}$$

where d_i denotes the distance between the UAV and the ith CAV, A and α denote the excess path loss offset and the path loss exponent, respectively, while $\eta \sim \mathcal{N}(0, \sigma_s^2)$ is the log-normal shadowing component, with variance σ_s^2. The multipath channel impulse response matrix is modeled as

$$\mathbf{H} = \sum_{p=1}^{P} \beta_p \mathbf{a}_{\mathrm{UAV}}^{\mathrm{H}}(\theta_p) \mathbf{a}_{\mathrm{CAV}}^{\mathrm{H}}(\phi_p), \tag{6}$$

where $\beta_p \sim \mathcal{CN}(0, \sigma_p^2)$ denotes the complex amplitude of the pth path, such that $\sum_p \sigma_p^2 = 1$, P is the number of multipath, ϕ_p and θ_p denote the angle of departure and angle of arrival, respectively, and $\mathbf{a}(\theta)$ is the normalized array function [22].

III. Performance assessment of UAV-assisted radio resource assignment

This section highlights the RRA procedures and how they impact the average access probability.

A. Radio Resources Assignment Algorithms

Two RRA algorithms are investigated accounting for the specific beamforming technique, the available radio resources at the UAVs, and the End-to-End (E2E) application latency requirement, which we denote by τ_{E2E}.

Let us consider a grid of time-frequency resources with $N_{\mathrm{ch}} \times N_{\mathrm{slot}}$, where N_{ch} denotes the number of frequency sub-channels and N_{slot} is the number of temporal slots. A similar architecture is used by the 5G NR Standard [18], where N_{ch} depends on the allocated bandwidth and $N_{\mathrm{slot}} \leq (\tau_{\mathrm{E2E}} / T_{\mathrm{slot}}) \, 0.5$ is defined according to the E2E latency requirement, with T_{slot} being the slot duration. Note that the product with 0.5 accounts for the resources to forward the data from the UAV to the receiving CAVs.

1) Fair RRA: The first approach, denoted as Fair RRA, ensures an even resource allocation between the set of beams and can be considered as a baseline. The number of time-frequency resources for the ℓth beam is

$$N_\ell^{(\mathrm{Fair})} = \left\lfloor \frac{N_{\mathrm{slot}} N_{\mathrm{ch}} N_{\mathrm{RF}}}{N_{\mathrm{beam}}} \right\rfloor, \tag{7}$$

where $N_{\mathrm{beam}} = |\mathcal{B}|$ is the cardinality of the UAV beamforming codebook.

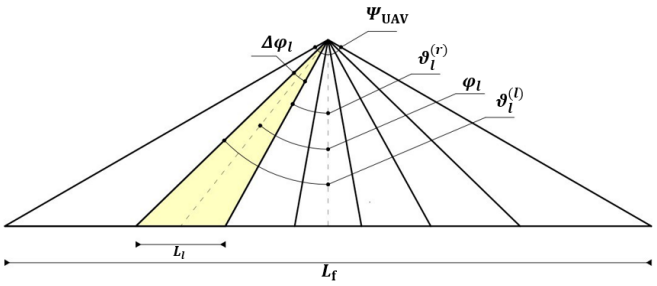

Fig. 2: Angles involved in the UAV beam footprint calculation.

2) Beam-based RRA: The second RRA approach considered, denoted as beam-based (BB) RRA, entails the distribution of resources among the various beams, taking into account the size of each specific beam footprint. Indeed, the larger the beam footprint, the higher the number of CAVs that will be covered and should be served. Accordingly, the number of time-frequency resources allocated for the ℓth beam is

$$N_\ell^{(\mathrm{BB})} = \left\lfloor N_{\mathrm{slot}} N_{\mathrm{ch}} N_{\mathrm{RF}} \frac{L_\ell}{L_{\mathrm{f}}} \right\rfloor, \tag{8}$$

where L_ℓ denotes the ℓth beam footprint such that $L_{\mathrm{f}} = \sum_{\ell=1}^{N_{\mathrm{beam}}} L_\ell$.

As depicted in Figure 2, the ℓth beam footprint can be computed geometrically as

$$L_\ell = h_{\mathrm{UAV}} \left| \tan\left(\vartheta_\ell^{(l)}\right) - \tan\left(\vartheta_\ell^{(r)}\right) \right|, \tag{9}$$

where $\vartheta_\ell^{(l)}$ and $\vartheta_\ell^{(r)}$ denote the left and right angle confining the ℓth beam, defined as

$$\begin{aligned} \vartheta_\ell^{(l)} &= \varphi_\ell - \frac{\Delta\varphi_\ell}{2} \\ \vartheta_\ell^{(r)} &= \varphi_\ell + \frac{\Delta\varphi_\ell}{2}, \end{aligned} \tag{10}$$

where φ_ℓ is the pointing direction of the ℓth beam, and $\Delta\varphi_\ell$ is the ℓth beamwidth, defined as

$$\Delta\varphi_\ell = \frac{2}{N_{\mathrm{UAV}} \cos(\varphi_\ell)}. \tag{11}$$

B. Average Access Probability Analysis

Herein, the objective is to analytically derive the average access probability, introduced in Sec. I, for a CAV seeking to establish communication with another CAV but facing a blocked V2V link, thereby exploiting relay through UAV.

Let us consider a highway road segment of length L_{f} with K lanes. The length of the road segment depends on the height of the UAV h_{UAV} and its covered field of view Ψ_{UAV}, and it can be computed as

$$L_{\mathrm{f}} = 2 \, h_{\mathrm{UAV}} \, \cos\left(\frac{\Psi_{\mathrm{UAV}}}{2}\right). \tag{12}$$

To determine the distribution of CAVs as a function of traffic density, we partition the highway road segment into spatial slots, each of size L_{v}, with the capacity to accommodate a single CAV. Consequently, L_{v} takes into consideration the

physical size of the CAV and allows for a minimum safety distance, assuming the scenario of maximum traffic congestion [23]. The maximum number of CAVs in the segment covered by the UAV is defined as $M^{(\max)} = \lfloor KL_{\rm f}/L_{\rm v} \rfloor$, while the maximum number of CAVs within the coverage area of the ℓth beam is expressed as $M_\ell^{(\max)} = \lfloor KL_\ell/L_{\rm v} \rfloor$. The probability that a spatial slot is occupied by a CAV can be obtained assuming a Point Poisson distribution over a single slot length, as

$$P_{\rm o} = \lambda L_{\rm v} e^{-\lambda L_{\rm v}}, \tag{13}$$

where λ is the vehicle density. It is evident that if $M_\ell^{(\max)} \leq N_\ell$, $\forall \ell$, the UAV is capable of granting access to all incoming requests for relay services. Conversely, the average access probability is computed as

$$P^{(\rm ACC)} = \sum_{\ell=1}^{N_{\rm beam}} \frac{P_\ell^{(\rm ACC)} = \text{Prob}\left(\overline{M}_\ell \leq N_\ell\right)}{N_{\rm beam}}, \tag{14}$$

where $\overline{M}_\ell$ denotes the number of valid relaying requests for the ℓth beam and N_ℓ is the maximum number of resources available for the ℓth beam, according to the RRA strategy in (7) and (8). Herein, we define a relaying request from the ith CAV as a valid request if $\text{SNR}_i \geq \gamma_{\rm th}$. The probability of having a valid request can be computed as

$$P_\ell^{(\rm VR)} = \text{Prob}\left(\text{SNR}_\ell \geq \gamma_{\rm th}\right), \tag{15}$$

where SNR_ℓ is the average SNR within the ℓth footprint, and $\gamma_{\rm th}$ is a threshold depending on the QoS requirements. By the central limit theorem, the distribution of the average SNR in dB can be approximated as $\text{SNR}_\ell \sim \mathcal{N}(\mu_\ell, \sigma_\ell^2)$, where the mean value μ_ℓ is computed using the path loss model in (5) considering the barycenter of the ℓth footprint, and the variance is $\sigma_\ell^2 = \sigma_s^2 + \sigma_n^2$ [6], [24]. Hence, the probability of a valid request is given by

$$P_\ell^{(\rm VR)} = Q\left(\frac{\gamma_{\rm th} - \mu_\ell}{\sigma_\ell}\right), \tag{16}$$

where $Q(\cdot)$ is the Q-function.

Through the discretization of space within each footprint, we can compute the probability of access employing a combinatorial methodology. The rationale behind this approach is straightforward: with a total of $M_\ell^{\max}$ spatial slots available, the likelihood of the mth slot being occupied is determined by the computed probability $P_{\rm o}$ in Equation (13), while the probability of a CAV in the mth slot issuing a valid request is represented by $P_\ell^{(\rm VR)}$, as indicated in Equation (16). Hence, the probability of access can be derived utilizing Equation (17).

IV. Numerical Results

This section presents the numerical results on the average access probability of a user as a function of both the UAV altitude and the vehicle density and the performance comparison between the two RRA techniques proposed. This comparison covers various scenarios, including different SNR thresholds and varying traffic conditions. In this context, we evaluate and compare the number of vehicles with an SNR above the threshold (connected vehicles) to the actual number of covered vehicles that have resources assigned (served vehicles) when both the RRA methods are used. The mathematical model results are validated via comparison with simulation results. The simulations were conducted in the MATLAB environment using parameters summarized in Table I. The simulated scenario faithfully replicates the description in Section II, with the sole distinction being the consideration of the actual SNR between the drone and CAV, as per Equation (4). In contrast, in the mathematical model, we assume vehicles under the same beam are characterized by the same SNR, as outlined in Section III-B.

TABLE I: Input Parameters

Parameter	Notation	Value
CAV's antenna elements	$N_{\rm UE}$	4
UAV's antenna elements	$N_{\rm UAV}$	8
RF chains	$N_{\rm RF}$	4
CAV's transmitting power	P_i	23 [dBm]
Noise power	σ_n^2	-101 [dBm]
Excess path loss offset	A	84.64 [dB]
Path loss exponent	α	1.55
Log-normal shadowing variance	σ_s^2	4
Number of lanes	K	5
UAV's Field of View	$\Psi_{\rm UAV}$	120°
Vehicle's average length	$L_{\rm v}$	5 [m]
Vehicle density	λ	40, 80 [cars/km]
SNR threshold	$\gamma_{\rm th}$	5, 10 [dB]
Carrier frequency	f_o	28 GHz
Number of frequency subchannels	$N_{\rm ch}$	2
Slot duration	$T_{\rm slot}$	125 [μs]
E2E max Delay	$\tau_{\rm E2E}$.	10 [ms] - as in [4]

In Figure 3a, we report the average access probability as a function of the UAV altitude. The curves were generated by maintaining a traffic density λ constant at 40 cars/km and varying the SNR threshold, $\gamma_{\rm th}$. In all the cases, the model's validity is confirmed by the near-perfect overlap of all four simulation curves with their respective theoretical counterparts (dashed curves). Looking at the two couples of curves in Figure 3a, it is clear how the gap between the performance of the two RRA algorithms varies depending on $\gamma_{\rm th}$. Specifically, when the SNR threshold is equal to 10 dB, both RRAs exhibit identical values of the average access probability. This suggests that, with such a high threshold, a significant portion of users is unable to access the network due to coverage limitations. Consequently, the number of users demanding resources becomes limited. As a result, both the beam-based RRA and the fair RRA effectively manage this reduced user population. When we increase the SNR threshold to 5 dB, we can observe a significant improvement in performance when adopting the beam-based approach. In this case, more users will have coverage, and this is especially true as the drone's altitude increases because the beams footprints of the various beams will be larger and can accommodate more users. Hence, the beam-based RRA stands out as the ideal algorithm to manage this heightened demand effectively. Concerning the overall decreasing trend observed, it is evident that as the drone's altitude increases, the radio link quality progressively deteriorates. Consequently, the average access probability, which represents the likelihood that

$$P_\ell^{(\mathrm{ACC})} = \sum_{m=1}^{N_\ell} \binom{M_\ell^{\max}}{m} \left(P_\mathrm{o}\, P_\ell^{(\mathrm{VR})}\right)^m \left(1 - P_\mathrm{o}\, P_\ell^{(\mathrm{VR})}\right)^{M_\ell^{\max}-m} \tag{17}$$

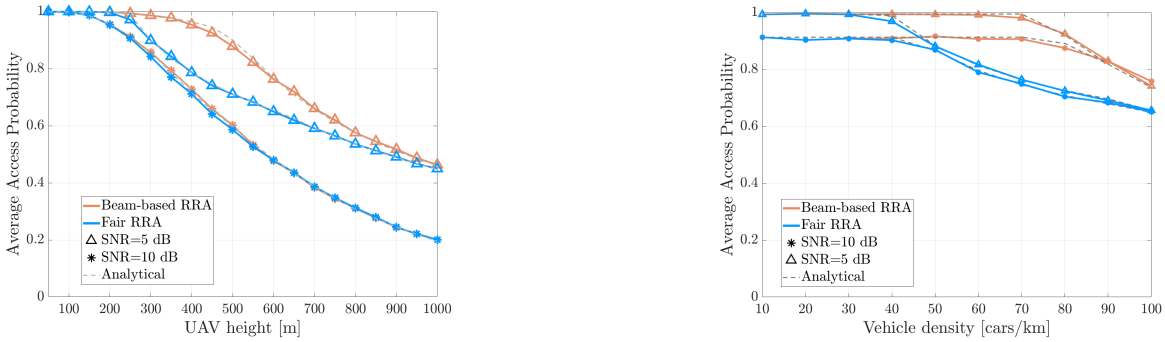

(a) (b)

Fig. 3: Comparison of average access probability versus UAV height (a) and vehicle density (b) for different conditions.

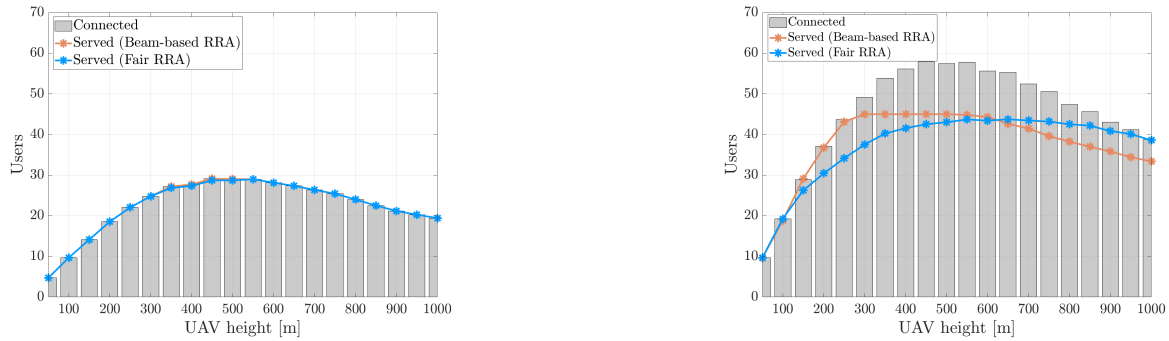

(a) $\lambda = 40$, SNR=10 dB. (b) $\lambda = 80$, SNR=10 dB.

Fig. 4: Connected users versus served users with both RRAs.

vehicles are adequately covered and receive sufficient resources, decreases sharply due to adverse radio conditions. For an SNR threshold of 10 dB, in order to meet the requirement of achieving a 99% average access probability, the drone should fly at an altitude of 150 meters. If we reduce the SNR threshold to 5 dB, then with the fair RRA, the UAV should operate at an altitude of 240 meters, whereas with the beam-based RRA, it should be at 350 meters. From this information, if our goal is to provide V2X service for a specific highway road segment, taking into account that the footprints of adjacent drones do not overlap, we can then derive the number of drones needed to effectively cover that particular stretch.

The superiority of the beam-based RRA becomes even more apparent when we plot the average access probability against varying vehicle density, as shown in Figure 3b. The two pairs of curves correspond to the two previously mentioned SNR scenarios, 5 dB and 10 dB. Here, we set the drone's altitude at 250 meters. Consequently, with a 10 dB SNR threshold, the average access probability never exceeds 91%. However, with a 5 dB threshold, we achieve good performance, at least until the vehicle density surpasses 70 cars/km.

Figure 4a illustrates the comparison between the number of connected users (grey barplot) and the users effectively served controlling the UAV altitude. The blue curve represents the fair RRA, while the orange curve represents the beam-based RRA. In this scenario, we maintain a constant SNR of 10 dB and a λ value of 40. This figure highlights a peak in connected users with increasing altitude. As the drone's altitude rises, its beams cover a larger area, accommodating more users. However, beyond a certain maximum altitude, the number of connected users declines due to deteriorating link quality, especially in the outermost beams. In this scenario, neither RRA outperforms the other, for the reasons discussed earlier.

To better appreciate the distinction between the two RRA curves, we have doubled the value of lambda from 40 to 80 cars/km, thus moving to a higher CAVs density scenario, as in Figure 4b. Here, we can observe two phenomena: firstly, the beam-based approach outperforms the fair RRA. However, beyond a certain UAV's height, the situation reverses. At very high altitudes, the side beams, although populated by a large number of users, may struggle to establish connections. As a result, most users requiring resources are concentrated in the central beams. Since the fair RRA allocates the same number of resources to all beams (with more resources assigned to

central beams than the beam-based approach), it shows better performance in this specific context.

V. Conclusions

In this paper, by leveraging on beamforming-enabled UAVs as relay nodes, we have proposed a robust solution to ensure dependable data exchange, even in scenarios where direct V2V communication faces hindrances. The introduction of the novel performance metric, the average access probability, has provided a nuanced understanding of the satisfaction level among vehicles covered by a drone's beam during resource requests for uplink traffic demands. This metric serves as a crucial indicator for evaluating the efficacy of the proposed system. Our contribution extends to the introduction of optimized RRA algorithms tailored for UAVs. These algorithms consider several factors, including beamforming, resource availability, user distribution, and application latency requirements. The numerical results validate the proposed model, emphasizing the pivotal role of access probability in optimizing system parameters such as UAV altitude and the number of drones. This work, therefore, not only addresses the challenges inherent in V2V communication but also presents a concrete framework for enhancing QoS in V2X sidelink communications. The findings of this study pave the way for further advancements in the integration of UAVs as relay nodes, contributing significantly to the realization of safer and more efficient connected vehicular networks.

Acknowledgment

This article was supported by the European Union under the Italian National Recovery and Resilience Plan (NRRP) of NextGenerationEU, partnership on "Telecommunications of the Future" (PE00000001 - program "RESTART", Structural Project 6GWINET). Furthermore, it is based upon work from COST Action INTERACT, CA20120, supported by COST (European Cooperation in Science and Technology).

References

[1] A. Bazzi, A. O. Berthet, C. Campolo, B. M. Masini, A. Molinaro, and A. Zanella, "On the design of sidelink for cellular v2x: A literature review and outlook for future," *IEEE Access*, vol. 9, pp. 97 953–97 980, 2021.

[2] I. Kilanioti, G. Rizzo, B. M. Masini, A. Bazzi, D. P. M. Osorio, F. Linsalata, M. Magarini, D. Löschenbrand, T. Zemen, and A. Kliks, "Intelligent transportation systems in the context of 5g-beyond and 6g networks," in *2022 IEEE Conference on Standards for Communications and Networking (CSCN)*, 2022, pp. 82–88.

[3] D. Mishra, A. Trotta, M. Di Felice, and E. Natalizio, "Performance analysis of multi-hop communication based on 5g sidelink for cooperative uav swarms," in *2021 IEEE International Mediterranean Conference on Communications and Networking (MeditCom)*, 2021, pp. 395–400.

[4] 5GAA Automotive Association, "C-v2x use cases volume iii: Examples and service level requirements," 5GAA c/o MCI Munich, Neumarkter Str. 21, 81673 München, Germany, Tech. Rep., January 2023, copyright © 2023 5GAA. All Rights Reserved. Version 1. Approved by 5GAA Board on December 19, 2022. [Online]. Available: https://www.5gaa.org

[5] J. Li, Y. Niu, H. Wu, B. Ai, R. He, N. Wang, and S. Chen, "Joint optimization of relay selection and transmission scheduling for uav-aided mmwave vehicular networks," *IEEE Transactions on Vehicular Technology*, vol. 72, no. 5, pp. 6322–6334, 2023.

[6] F. Linsalata, S. Mura, M. Mizmizi, M. Magarini, P. Wang, M. N. Khormuji, A. Perotti, and U. Spagnolini, "Los-map construction for proactive relay of opportunity selection in 6g v2x systems," *IEEE Transactions on Vehicular Technology*, vol. 72, no. 3, pp. 3864–3878, 2023.

[7] D. Tian, J. Zhou, Z. Sheng, M. Chen, Q. Ni, and V. C. M. Leung, "Self-organized relay selection for cooperative transmission in vehicular ad-hoc networks," *IEEE Transactions on Vehicular Technology*, vol. 66, no. 10, pp. 9534–9549, 2017.

[8] P. Wang, J. Fang, X. Yuan, Z. Chen, and H. Li, "Intelligent reflecting surface-assisted millimeter wave communications: Joint active and passive precoding design," *IEEE Transactions on Vehicular Technology*, vol. 69, no. 12, pp. 14 960–14 973, 2020.

[9] P. Pourbaba, K. B. S. Manosha, S. Ali, and N. Rajatheva, "Full-duplex uav relay positioning for vehicular communications with underlay v2v links," in *2019 IEEE 89th Vehicular Technology Conference (VTC2019-Spring)*, 2019, pp. 1–6.

[10] F. D. S. Moulin, C. Wiame, C. Oestges, and L. Vandendorpe, "Stochastic geometry-based modelling of mobile uav relay networks under realistic fading," in *2021 IEEE 93rd Vehicular Technology Conference (VTC2021-Spring)*, 2021, pp. 1–7.

[11] T. A. Kiet, N. T. L. Quyen, H. P. Hieu, and V. T. Hung, "A novel approach for uav-aided vehicle-to-everything networks," in *2022 16th International Conference on Ubiquitous Information Management and Communication (IMCOM)*, 2022, pp. 1–4.

[12] Y. Kawamoto, T. Mitsuhashi, and N. Kato, "Uav-aided information diffusion for vehicle-to-vehicle (v2v) in disaster scenarios," *IEEE Transactions on Emerging Topics in Computing*, vol. 10, no. 4, pp. 1909–1917, 2022.

[13] I. Rzig, W. Jaafar, M. Jebalia, and S. Tabbane, "Uav-assisted computation offloading in vehicular networks," in *2023 IEEE International Performance, Computing, and Communications Conference (IPCCC)*, 2023, pp. 236–241.

[14] H. Wu, F. Lyu, C. Zhou, J. Chen, L. Wang, and X. Shen, "Optimal uav caching and trajectory in aerial-assisted vehicular networks: A learning-based approach," *IEEE Journal on Selected Areas in Communications*, vol. 38, no. 12, pp. 2783–2797, 2020.

[15] M. Khabbaz, J. Antoun, and C. Assi, "Modeling and performance analysis of uav-assisted vehicular networks," *IEEE Transactions on Vehicular Technology*, vol. 68, no. 9, pp. 8384–8396, 2019.

[16] J. Li, Y. Niu, H. Wu, B. Ai, R. He, N. Wang, and S. Chen, "Joint optimization of relay selection and transmission scheduling for uav-aided mmwave vehicular networks," *IEEE Transactions on Vehicular Technology*, vol. 72, no. 5, pp. 6322–6334, 2023.

[17] F. Conserva and R. Verdone, "Analytical description of access probability and rra strategy for uav-aided vehicular applications," in *Proceedings of the Ninth Workshop on Micro Aerial Vehicle Networks, Systems, and Applications*, ser. DroNet '23. New York, NY, USA: Association for Computing Machinery, 2023, p. 21–26. [Online]. Available: https://doi.org/10.1145/3597060.3597241

[18] 3GPP, "Nr; nr and ng-ran overall description; stage 2 (release 17)," 3rd Generation Partnership Project (3GPP), Technical Specification (TS) 38.300, 04 2022, version 17.4.0.

[19] F. Morandi, F. Linsalata, M. Brambilla, M. Mizmizi, M. Magarini, and U. Spagnolini, "A probabilistic codebook technique for fast initial access in 6g vehicle-to-vehicle communications," in *2021 IEEE International Conference on Communications Workshops (ICC Workshops)*, 2021, pp. 1–6.

[20] D. Yang, L.-L. Yang, and L. Hanzo, "Dft-based beamforming weight-vector codebook design for spatially correlated channels in the unitary precoding aided multiuser downlink," in *2010 IEEE International Conference on Communications*, 2010, pp. 1–5.

[21] H. Shakhatreh, W. Malkawi, A. Sawalmeh, M. Almutiry, and A. Alenezi, "Modeling ground-to-air path loss for millimeter wave uav networks," 2021.

[22] M. Mizmizi, D. Tagliaferri, D. Badini, C. Mazzucco, and U. Spagnolini, "Channel estimation for 6g v2x hybrid systems using multi-vehicular learning," *IEEE Access*, vol. 9, pp. 95 775–95 790, 2021.

[23] K. Dong, M. Mizmizi, D. Tagliaferri, and U. Spagnolini, "Vehicular blockage modelling and performance analysis for mmwave v2v communications," in *ICC 2022 - IEEE International Conference on Communications*, 2022, pp. 3604–3609.

[24] S. Mignardi, D. Ferretti, R. Marini, F. Conserva, S. Bartoletti, R. Verdone, and C. Buratti, "Optimizing beam selection and resource allocation in uav-aided vehicular networks," in *2022 Joint European Conference on Networks and Communications & 6G Summit (EuCNC/6G Summit)*, 2022, pp. 184–189.